

Platelet-targeted thrombolysis for treatment of acute ischemic stroke

Jason S. Palazzolo,¹ Anukreity Ale,¹ Heidi Ho,² Shweta Jagdale,¹ Brad R. S. Broughton,³ Robert L. Medcalf,² David K. Wright,⁴ Karen Alt,⁵ Christoph E. Hagemeyer,^{1,*} and Be'eri Niego^{1,*}

¹NanoBiotechnology Laboratory and ²Molecular Neurotrauma and Haemostasis, Australian Centre for Blood Diseases, Central Clinical School, Monash University, Melbourne, VIC, Australia; ³Department of Pharmacology, Monash Biomedicine Discovery Institute, ⁴Department of Neuroscience, Central Clinical School, and ⁵NanoTheranostics Laboratory, Australian Centre for Blood Diseases, Central Clinical School, Monash University, Melbourne, VIC, Australia

Key Points

- Platelet-targeted thrombolysis with SCE5-scuPA achieved favorable outcomes vs tenecteplase-tPA in 2 mouse models of ischemic stroke.
- Thrombolytic strategies that harness activated platelets for drug targeting better suit the platelet-rich nature of stroke-causing thrombi.

Thrombolysis with tissue-type plasminogen activator (tPA) remains the main treatment for acute ischemic stroke. Nevertheless, tPA intervention is limited by a short therapeutic window, low recanalization rates, and a risk of intracranial hemorrhage (ICH), highlighting the clinical demand for improved thrombolytic drugs. We examined a novel thrombolytic agent termed “SCE5-scuPA,” comprising a single-chain urokinase plasminogen activator (scuPA) fused with a single-chain antibody (SCE5) that targets the activated glycoprotein IIb/IIIa platelet receptor, for its effects in experimental stroke. SCE5-scuPA was first tested in a whole blood clot degradation assay to show the benefit of platelet-targeted thrombolysis. The tail bleeding time, blood clearance, and biodistribution were then determined to inform the use of SCE5-scuPA in mouse models of photothrombotic stroke and middle cerebral artery occlusion against tenecteplase. The impacts of SCE5-scuPA on motor function, ICH, blood–brain barrier (BBB) integrity, and immunosuppression were evaluated. Infarct size was measured by computed tomography imaging and magnetic resonance imaging. SCE5-scuPA enhanced clot degradation *ex vivo* compared with its nonplatelet-targeting control. The maximal SCE5-scuPA dose that maintained hemostasis and a rapid blood clearance was determined. SCE5-scuPA administration both before and 2 hours after photothrombotic stroke reduced the infarct volume. SCE5-scuPA also improved neurologic deficit, decreased intracerebral blood deposits, preserved the BBB, and alleviated immunosuppression poststroke. In middle cerebral artery occlusion, SCE5-scuPA did not worsen stroke outcomes or cause ICH, and it protected the BBB. Our findings support the ongoing development of platelet-targeted thrombolysis with SCE5-scuPA as a novel emergency treatment for acute ischemic stroke with a promising safety profile.

Introduction

Acute ischemic stroke (AIS) is one of the leading causes of disability and death worldwide.¹ Thrombolytic therapy, a long-established intervention for the treatment of AIS, involves the systemic administration of tissue-type plasminogen activator (tPA).^{2,3} Thrombolysis offers stroke patients several advantages, mainly in its simplicity and “real-life” applicability compared with invasive endovascular clot retrieval that requires expert personnel and resources not readily available, particularly for rural and remote populations.^{4,5}

Submitted 29 November 2021; accepted 9 April 2022; prepublished online on *Blood Advances* First Edition 28 April 2022. <https://doi.org/10.1182/bloodadvances.2021006691>.

*C.E.H. and B.N. are joint senior authors.

Requests for data sharing may be submitted to the corresponding author (e-mail: beeri.niego@monash.edu).

The full-text version of this article contains a data supplement.

© 2023 by The American Society of Hematology. Licensed under [Creative Commons Attribution-NonCommercial-NoDerivatives 4.0 International \(CC BY-NC-ND 4.0\)](https://creativecommons.org/licenses/by-nc-nd/4.0/), permitting only noncommercial, nonderivative use with attribution. All other rights reserved.

However, the current clinical regimen of tPA therapy faces several limitations such as a narrow therapeutic window (4.5 hours post-stroke onset)^{6,7} and a short circulating half-life (4-6 minutes)^{8,9} that require tPA to be infused over a 1-hour period. tPA also increases the risk of hemorrhagic transformation,^{10,11} disrupts the blood–brain barrier (BBB),¹² and possibly exacerbates immunosuppression.^{13,14} Compounding these limitations is that tPA is associated with low rates of recanalization (~40%),^{15,16} which is often attributed to the platelet-rich composition of arterial thrombi.¹⁷

Platelet-rich clots, in addition to minimizing the accessibility of tPA to fibrin¹⁸ and disrupting its fibrin-dependent mode of plasminogen activation (PA), are also increased in rigidity.¹⁷ Furthermore, platelets secrete plasminogen activator inhibitor-1 (PAI-1) and, hence, platelet-rich thrombi possess an overwhelming inhibitory capacity of any PA.^{19,20} Collectively, these traits contribute to the thrombolytic resistance frequently observed in platelet-rich clots that is particularly relevant in the context of tPA treatment of AIS.

Tenecteplase (TNK-tPA), a genetically modified, full-length tPA variant with a longer half-life (~20 minutes) and bolus administration,²¹ represents a new benchmark for thrombolysis.²² However, there are inconsistent reports regarding its superior efficacy and safety profiles compared with its parental enzyme.²³

To address the current shortfalls of tPA and TNK-tPA, we investigated a novel thrombolytic strategy for AIS designed to exploit the platelet-rich nature of arterial thrombi to increase the clot-busting capability of a given PA. Specifically, a platelet-targeted therapeutic candidate was assessed,²⁴ comprising a single-chain urokinase plasminogen activator (scuPA) fused with a single-chain antibody (SCE5) that targets the activated conformation of the glycoprotein IIb/IIIa receptor complex, presented exclusively on activated platelets.^{25–27} The resulting recombinant protein (or fusion construct), termed “SCE5-scuPA,” has been previously tested in general models of thrombosis²⁴ but never in AIS. Here, we describe fundamental *ex vivo* and *in vivo* characterization studies of SCE5-scuPA, which informed its first evaluation in both a cortical photothrombotic mouse model and a mechanical middle cerebral artery occlusion (MCAo) mouse model of AIS. Beneficial outcomes of this innovative thrombolytic approach in stroke are presented.

Methods

Fusion construct production and purification

The production, purification, and characterization according to flow cytometry and activity assays of SCE5-scuPA and the nonplatelet-targeting fusion construct control (mut-scuPA) were performed as described by Wang et al.²⁴ mut-scuPA possessed the same scuPA component fused to a scrambled single-chain antibody, which removed any antigenic binding capacity. Detailed methods of the fusion construct production, purification, and bio-functionality validation (platelet flow cytometry and urokinase enzymatic activity assays) are available in the supplemental Materials.

Ex vivo whole blood clot degradation “halo” assay

Naive whole blood. The experimental use of human blood was approved by the Monash University Human Research Ethics Committee (Project 67/15). The clot degradation (or “halo”) protocol followed the methodology described by Bonnard et al.²⁸ In brief, whole blood from healthy donors was collected as described in the

supplemental Materials. The blood (25 μ L) was mixed with a clotting mixture (5 μ L) containing 15% (vol/vol) Dade Innovin (Siemens Healthineers), 67 mM CaCl₂ buffered with *N*-2-hydroxyethylpiperazine-*N*'-2-ethanesulfonic acid (25 mM *N*-2-hydroxyethylpiperazine-*N*'-2-ethanesulfonic acid, 137 mM NaCl) to produce halo-shaped clots in 96 wells that were allowed to form for 1 hour at 37°C.

Reconstituted whole blood. The halo assay²⁸ was further modified to study the clot lysis profiles of SCE5-scuPA and mut-scuPA across blood clots with a platelet-concentration gradient. Naive whole blood was first centrifuged at room temperature for 10 minutes, as described in the flow cytometry protocol discussed earlier. The platelet-rich plasma (PRP) and red blood cells (RBCs) were isolated by using low-shear pipetting and stored separately at room temperature. A sample of the PRP was retained, and the remainder was centrifuged at room temperature for 7 minutes at 1700 RCF (acceleration/deceleration set to 10/0, respectively) to produce platelet-poor plasma (PPP). The PPP supernatant was collected carefully (to not disturb the pellet) and kept at room temperature.

Having isolated the RBCs, PRP, and PPP, the 3 components were mixed across 7 different reconstituted blood mixtures (labeled Clots 1-7). Across each mixture, the proportion of RBCs was kept constant at 40% (reflective of typical human hematocrit levels²⁹), whereas the proportion of PRP and PPP was varied to produce a platelet-concentration gradient in which Clot 1 contained the most platelets and Clot 7 contained the least, as shown in supplemental Table 1. Once the reconstituted whole blood mixtures were prepared, automated platelet counts were performed with a CELL-DYN Emerald analyzer (Abbott) before they were applied to the same halo assay protocol described earlier.

Spectrophotometric measurements and analysis. Once clots were formed, 70 μ L of either 100 nM SCE5-scuPA or mut-scuPA was added. The plate was then analyzed on the FLUOstar OPTIMA microplate (BMG Labtech) reader set to 37°C, measuring absorbance at 492 nm for 3 hours in 1-minute intervals (with no shaking). Using negative and positive controls (no fusion construct [A_{zero}] and no clotting mixture [A_{total}], respectively), the percentage of clot degradation at each time-point [Dx(t)] was calculated from the corresponding absorbance value [Ax(t)] according to the formula:

$$Dx(t) = \frac{Ax(t) - Azero(t)}{Atotal(t) - Azero(t)} \cdot 100$$

The time elapsed for 50% clot degradation was then obtained by fitting the curve to a sigmoidal, 4PL, log(concentration) nonlinear regression followed by interpolation of the time to 50% degradation. In addition, the maximal clot lysis rate (CLR_{max}) and the time elapsed for clot degradation to initiate (activation time [A_t]) were calculated from the percent clot degradation curve by extraction of the maximal first derivative value (CLR_{max}) and the first time point where the first derivative value was $>1.5 (A_t)$, respectively.²⁸

In vivo studies

Male C57BL6/J mice aged 8 to 12 weeks were used in all experimentation. All animal studies were approved by the Alfred Research Alliance Animal Ethics Committee (AEC approval numbers E/1534/2015/B, E/1625/2016/M, and E/1667/2016/M). Animals were sourced from the Precinct Animal Centre, Monash

Animal Research Platform, and Melbourne Bioresources Platform. Detailed descriptions of the in vivo methodologies are provided in the supplemental Materials.

Mouse tail bleeding safety investigation

The mouse tail bleeding assay was performed to identify the safest dose of SCE5-scuPA for subsequent in vivo investigations. Alongside the saline vehicle alone and 2.5 mg/kg TNK-tPA, ascending doses of SCE5-scuPA (75, 150, or 300 U/g) were tested. The total blood volume lost from a tail tip excision over 20 minutes was then determined to assess the impact of each SCE5-scuPA dosage on hemostasis as an indication of its safety.

In vivo blood clearance and biodistribution investigation

SCE5-scuPA was fluorescently labeled with NHS-Cy7.5 dye and then studied in vivo for its pharmacokinetic properties. The biodistribution and blood clearance profiles of SCE5-scuPA were determined from collected organs and blood samples, respectively, up to 4 hours postinjection. Quantification of fluorescence was performed with the Odyssey near-infrared fluorescent scanner (LI-COR Biosciences).

Photothrombotic ischemic stroke model

A photothrombotic stroke was induced in the right primary motor cortex (M1 region) of mice, as previously described.^{30,31} In the main study, just before stroke induction, the mice were intravenously (IV) administered saline vehicle alone, 150 U/g SCE5-scuPA, 2.5 mg/kg TNK-tPA, 2 µg/g SCE5 (alone), or 150 U/g mut-scuPA. The neurologic deficit was assessed at 1 and 3 days poststroke. In a subcohort of animals, mice were intracardially perfused at 3 days. Brains were then homogenized and biochemically examined for albumin extravasation and hemoglobin content as an indication of BBB breakdown and cerebral hemorrhage/thrombolytic efficacy, respectively. The brains of the remaining cohort were scanned by computed tomography (CT) imaging at 7 days and analyzed for infarct volumes and cerebral blood deposits (supplemental Materials). Blood cell counts at both time points, as well as spleen weight at day 3, were also recorded to determine any systemic immunologic impact poststroke. A single blinded operator performed all surgeries, treatments, and neurologic deficit assessments.

To better simulate clinical thrombolysis, we then performed a separate study in which interventions were delivered IV 2 hours postcortical photothrombosis (saline, 75 U/g SCE5-scuPA, or 75 U/g of the nontargeted mut-scuPA control). The neurologic deficit and weight loss were assessed 24 hours poststroke, followed by euthanasia, intracardial perfusion, and evaluation of infarct volume by postmortem (in skull) magnetic resonance imaging (MRI). The blood, plasma, spleen, and brain homogenates were also analyzed as described in the main study noted earlier. The supplemental Materials provide details of the MRI scanning protocol and the various tests performed.

MCAo stroke model

Transient thread occlusion of the mouse MCA was performed over 45 minutes, as we recently described.¹³ Treatments were administered IV at reperfusion (saline, 150 U/g SCE5-scuPA, or 150 U/g

mut-scuPA). Outcomes were assessed 24 hours poststroke. Details are provided in the supplemental Materials.

Gelatin zymography

Details on the gelatin zymography technique are presented in the supplemental Materials.

Statistical analysis

All statistical analyses were performed by using GraphPad Prism version 9.0 software (GraphPad Software). Neuroscores were analyzed by using a nonparametric Kruskal-Wallis one-way analysis of variance with uncorrected Dunn's post hoc analysis, or by using the Mann-Whitney test. All other comparisons of parametric data with ≥ 3 groups were performed by standard one- or 2-way analyses of variance with post hoc tests adjusted for multiple comparisons, as stated in the figure legends. Comparisons between 2 groups of parametric data were performed by using a 2-tailed *t* test. A *P* value $< .05$ was considered significant. Outliers were detected by using the ROUT method ($Q = 1\%$) and excluded from the analyses. The figure captions provide exact details of the statistical analysis performed.

Results

Platelet-targeting function of SCE5-scuPA increases clot degradation efficacy ex vivo

Initial validation experiments of the SCE5-scuPA fusion construct by platelet flow cytometry and uPA activity assays confirmed an SCE5-mediated binding to activated platelet and thrombolytic activity of the scuPA portion, respectively (supplemental Figures 1 and 2). SCE5-scuPA was then tested on whole blood clots to assess the synergistic benefit of the platelet-targeted, scuPA-mediated plasminogen activation approach.

When applied to naive whole blood thrombi, SCE5-scuPA showed more efficient thrombolytic outcomes than the nonplatelet-targeting control (mut-scuPA), achieving a significantly faster time elapsed for 50% clot degradation ($P < .001$) (Figure 1C), greater CLR_{max} ($P < .05$) (Figure 1E), and, although not significantly different, a more rapid initiation of clot lysis (A_t) ($P = .053$) (Figure 1D). The experiment was then extended to study the fusion constructs ex vivo on modified blood clots with a platelet concentration gradient (ranging from 60% PRP [vol/vol; Clot 1] to no platelets [Clot 7]) (supplemental Figure 3A) but consistent levels of RBCs that ensured comparable levels of maximal absorbance (supplemental Figure 3B). As shown in Figure 1F, SCE5-scuPA achieved a significantly higher CLR_{max} on Clot 1 compared with Clots 5, 6, and 7. Interestingly, although SCE5-scuPA maintained a significantly greater CLR_{max} than mut-scuPA on platelet-rich clots (1, 2, and 4), it showed comparable CLR_{max} on platelet-poor clots (5, 6, and 7). Taken together, although limited by their ex vivo nature, these findings show the benefits of our platelet-targeted thrombolysis strategy for degradation of platelet-rich clots.

Dose escalation study for identification of a safe dose of SCE5-scuPA

Mice were administered increasing doses of SCE5-scuPA to identify the highest dosage that did not cause excessive bleeding from the tail vein. Although doses up to 150 U/g SCE5-scuPA

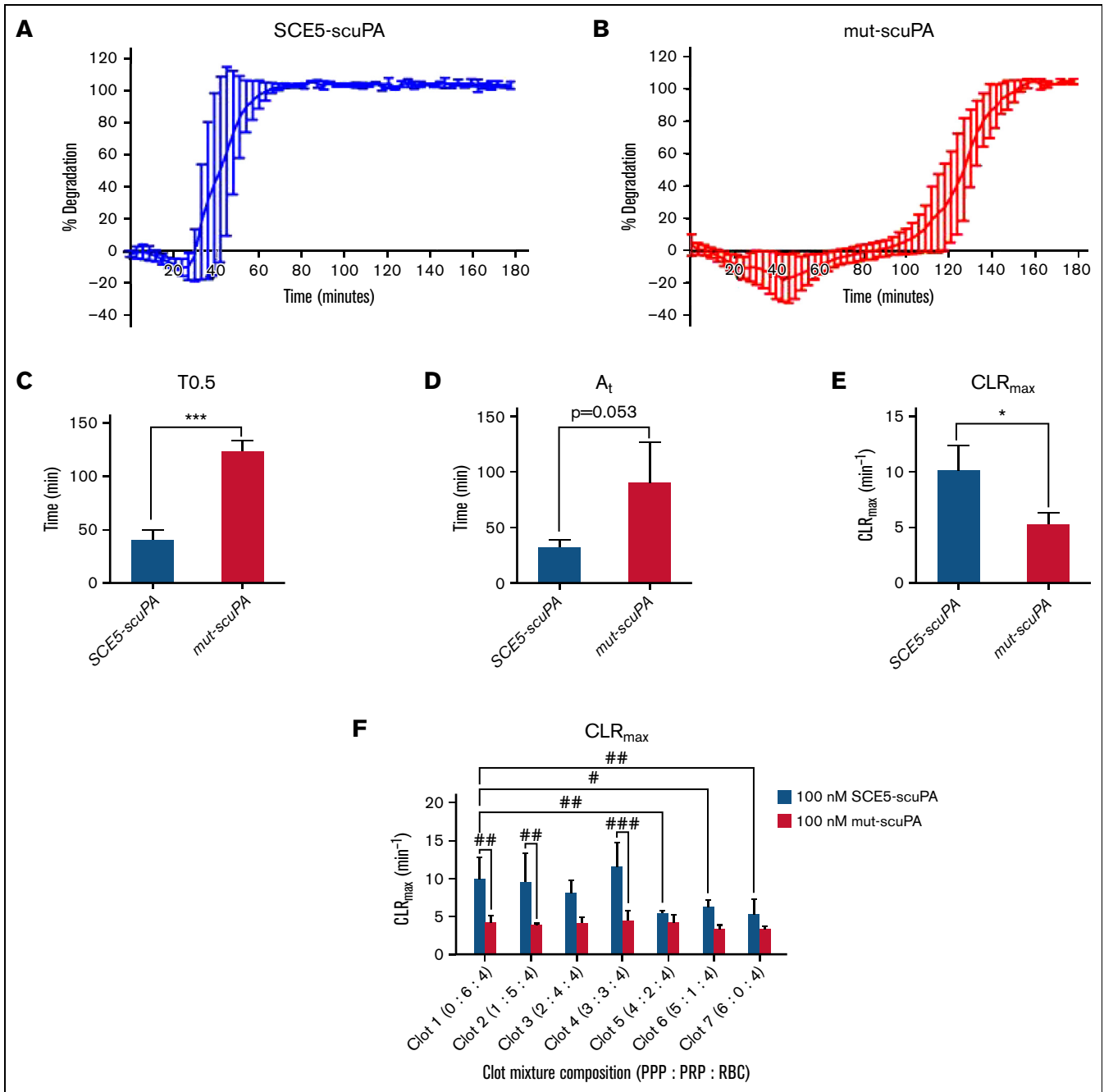


Figure 1. Activated platelet-targeting improves the clot lysis efficiency of SCE5-scuPA. (A and B) Collation of percent clot degradation curves of naive whole blood for 100 nM SCE5-scuPA (A) and nontargeted mut-scuPA control (B), respectively. (C) Fifty percent clot degradation time (T0.5). (D) Time until clot lysis initiation (A_t). (E) CLR_{max} achieved during clot lysis. (F) CLR_{max} calculated from 100 nM SCE5-scuPA and mut-scuPA on clots prepared with reconstituted whole blood mixtures with a platelet-concentration gradient (Clot 1 = 60% platelets [vol/vol]; Clot 7 = no platelets). All data presented as mean \pm standard deviation. $\#P < .05$, $\#\#\#P < .001$ by 2-way analysis of variance with Šidák's post hoc analysis. $*P < .05$, $***P < .001$ by a *t* test (unpaired, 2-tailed). $n = 3$.

yielded a blood volume loss comparable to that of vehicle-treated mice, administration of 300 U/g SCE5-scuPA resulted in a significantly greater blood loss than vehicle ($P < .05$) (Figure 2A). These findings suggest that a dose of 150 U/g SCE5-scuPA is the highest possible safe regimen that does not disrupt normal hemostasis. Interestingly, mice treated with 2.5 mg/kg TNK-tPA also exhibited a blood loss comparable to that in saline-treated

mice, indicating that the standard of care for our investigations did not disrupt hemostasis either and was safe in this regard.

Biodistribution and blood clearance of SCE5-scuPA

Biodistribution studies showed that SCE5-scuPA accumulated mostly in the spleen and liver at 4 hours postinjection, with

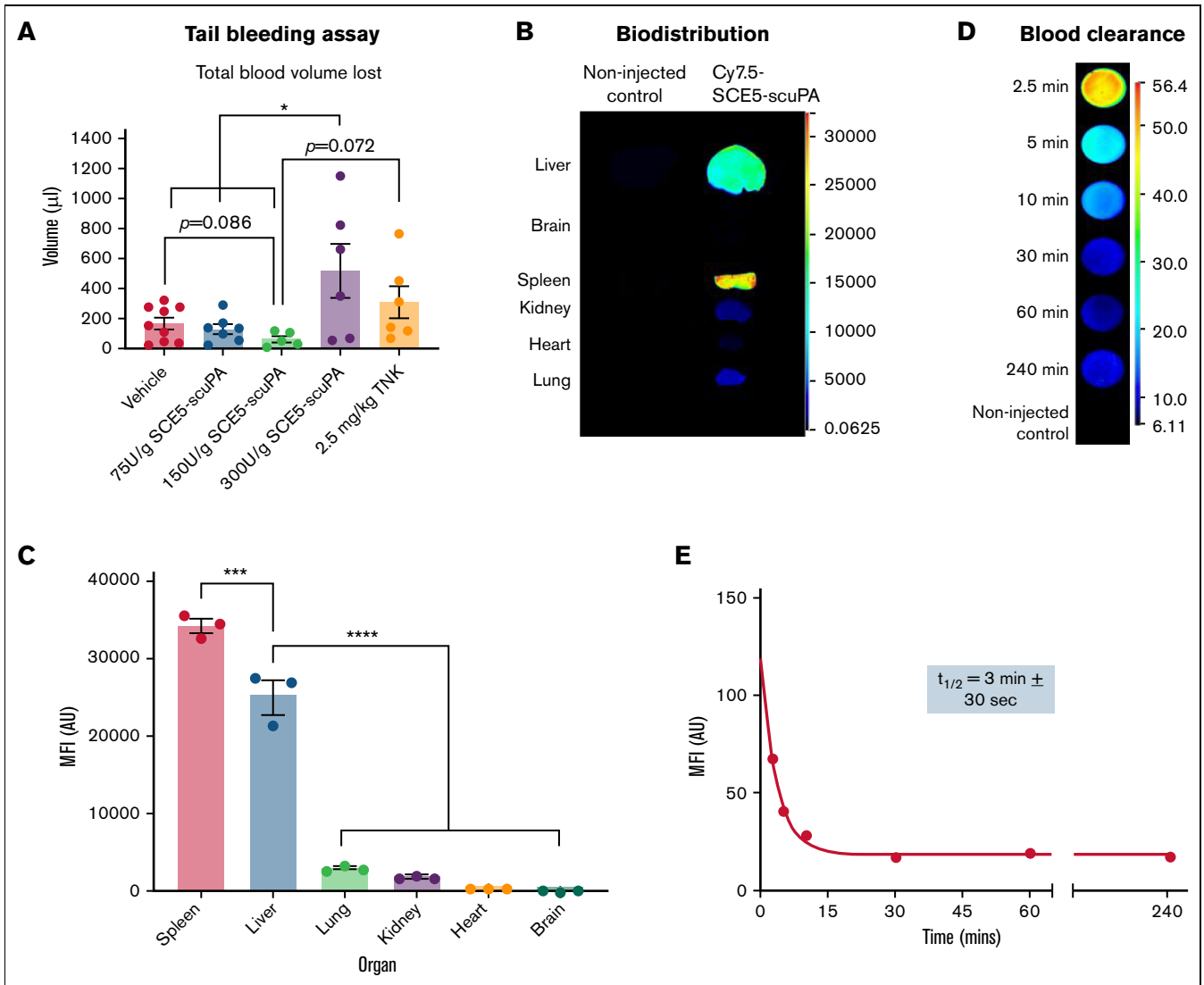


Figure 2. Hemostatic safety characterization, biodistribution, and pharmacokinetic parameters of SCE5-scuPA in the mouse. (A) Tail bleeding safety studies with SCE5-scuPA, showing the average total blood volume lost from a mouse tail wound over 20 minutes; 150 U/g is the highest SCE5-scuPA dose that does not disrupt hemostasis. $n = 5$ to 9. (B) Representative near-infrared fluorescence scans of perfused organs collected 4 hours after injection of Cy7.5-conjugated SCE5-scuPA (0.5 $\mu\text{g/g}$). (C) Quantification of the biodistribution of SCE5-scuPA by mean fluorescence intensity (MFI) per pixel in major organs. SCE5-scuPA predominately accumulates in the spleen and liver. $n = 3$. (D) Representative near-infrared fluorescence scans of blood samples collected at the designated time points. (E) Representative blood clearance plot of blood MFI per pixel vs time, fitted to a one-phase exponential decay nonlinear regression, after intravenous administration of Cy7.5-conjugated SCE5-scuPA (150 U/g). SCE5-scuPA is rapidly cleared from the circulation, with a half-life of 3 minutes \pm 30 seconds. $n = 4$. All data are presented as mean \pm standard error of the mean. * $P < .05$, *** $P < .001$, **** $P < .0001$ by one-way analysis of variance with Tukey's post hoc analysis. AU, arbitrary units.

negligible levels detected in the lung, kidney, heart, and brain tissues ($P < .0001$) (Figure 2B-C). In addition, pharmacokinetic investigations (Figure 2D-E) revealed that SCE5-scuPA has a rapid blood clearance profile, with an average circulating half-life of 3 minutes \pm 30 seconds (mean \pm standard error of the mean). Together with the tail bleeding studies, this thorough in vivo characterization informed the optimal design of our ensuing stroke studies with SCE5-scuPA (described in the following sections).

SCE5-scuPA improves neurologic deficit post-photothrombotic ischemic stroke

Neurologic deficit assessment revealed that administration of SCE5-scuPA immediately before stroke induction achieved significantly lower deficit scores compared with every other treatment cohort, across both 1 and 3 days poststroke ($P < .05$) (Figure 3A-B). A subcohort of vehicle-, SCE5-scuPA-, and TNK-TPA-treated mice were further tested for motor deficit using the

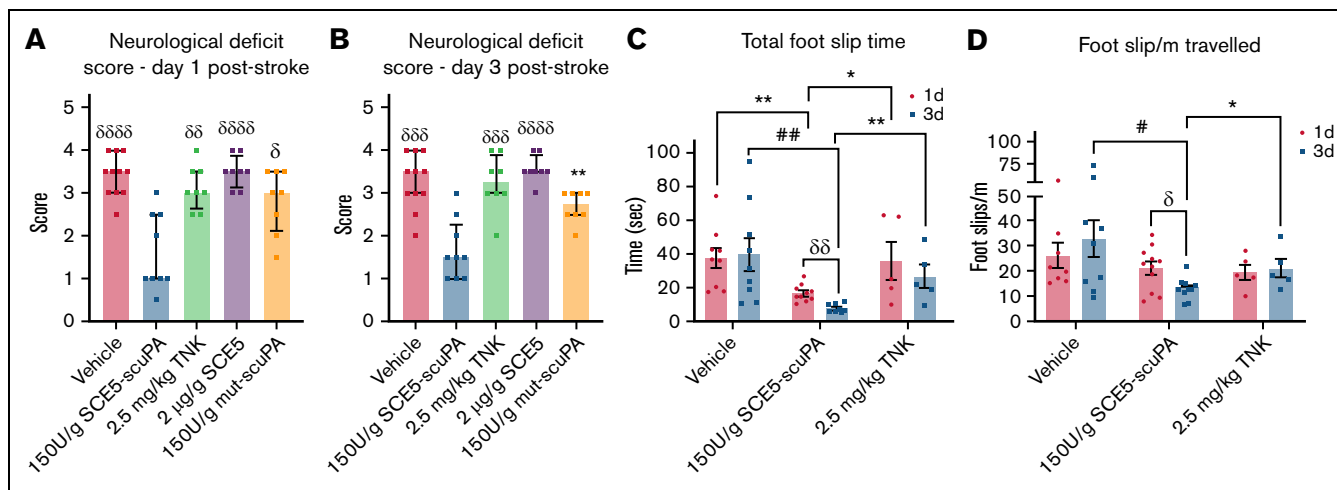


Figure 3. SCE5-scuPA, administered before photothrombotic stroke, improves the neurologic deficit after stroke. (A and B) Neurologic deficit scores at 1 and 3 days post-photothrombotic stroke, respectively. Median \pm interquartile range. $\delta P < .05$, $\delta\delta P < .01$, $\delta\delta\delta P < .001$, $\delta\delta\delta\delta P < .0001$ compared with SCE5-scuPA by a Kruskal-Wallis test with uncorrected Dunn's post hoc analysis. $**P < .01$ by a Mann-Whitney test (unpaired, 2-tailed). (C and D) Total cumulative foot slip time (C) and total foot slips per meter traveled (D). Mean \pm standard error of the mean. $\#P < .05$, $\#\#\#P < .01$ by 2-way analysis of variance with Tukey's post hoc analysis. $\delta P < .05$, $\delta\delta P < .01$ by a paired *t* test (2-tailed). $*P < .05$, $**P < .01$ by an unpaired *t* test (2-tailed). $n = 5-11$.

ANY-maze movement tracking apparatus (Stoelting Co.) that also measures foot slips (interpreted as motor skill errors). Notably, mice treated with SCE5-scuPA (just before stroke) displayed a better motor performance overall (Figure 3C-D). SCE5-scuPA was the only treatment to achieve improvement over time, with significant reduction in both total foot slip time (the average duration of each sensor activation; $P < .01$) (Figure 3C) and foot slips per meter ($P < .05$) (Figure 3D) at day 3 relative to day 1. Compared with mice treated with vehicle and TNK-tPA, SCE5-scuPA-treated mice also achieved significantly shorter total foot slip times on both days 1 and 3 (P as indicated), and reduced foot slips per meter traveled on day 3 poststroke ($P < .05$). It is worth noting that when treatment with SCE5-scuPA (75 U/g) at 2 hours poststroke was attempted, we did not observe a reduction in neurologic deficit 22 hours later (not shown). However, some benefits of the poststroke intervention could be observed, as the thrombolytic attenuated weight loss during these early, critical (≤ 24) hours after stroke (from $8.98 \pm 0.61\%$ with vehicle to $7.27 \pm 0.58\%$ with SCE5-scuPA; $n = 8-9$; $P = .062$ by *t* test; not shown).

SCE5-scuPA reduces cerebral infarction when administered before and after photothrombotic stroke

When examining parenchymal brain damage and bleeding 7 days after administration of SCE5-scuPA just before stroke, using our unique CT scanning protocol (Figure 4A), it became apparent that although TNK-tPA treatment reduced infarct volume compared with the vehicle (as expected), treatment with SCE5-scuPA was superior to TNK-tPA, resulting in significantly smaller infarct volumes relative to both vehicle- and TNK-tPA-treated mice ($P < .05$) (Figure 4B). Extending the analysis to measuring blood deposits within the infarcted brain tissue suggested that SCE5-scuPA treatment may also safely enhance clot lysis (and clearance) while minimizing brain bleeds compared with both vehicle- and TNK-tPA-treated mice; however, these results did not reach

significance ($P = .5173$ and $P = .4438$, respectively) (Figure 4C). Importantly, when examining the infarct volume by T2* MRI at 24 hours after stroke, with SCE5-scuPA administration at 2 hours poststroke (a protocol that resembles a clinical scenario), a significant 25% reduction in infarct size was achieved only by SCE5-scuPA (from 45.82 mm^3 on average with vehicle to 35.06 mm^3 with SCE5-scuPA) but not with its mutated control (both at 75 U/g; $P < .05$) (Figure 4D-E). Although infarct examinations at later time points are also warranted, these results together suggest that targeted thrombolysis may be superior to current thrombolytic strategies in its capacity to rescue brain tissue during stroke.

SCE5-scuPA treatment decreases albumin extravasation and hemoglobin content in brain tissue

Determination of brain albumin levels by using enzyme-linked immunosorbent assay, indicative of BBB breakdown poststroke, found that SCE5-scuPA-administered mice (treated at the time of stroke) presented with significantly less cerebral albumin compared with mice treated with vehicle alone ($P < .05$) (Figure 5A). Although not statistically significant, a trend was also apparent for reduced brain albumin with SCE5-scuPA relative to TNK-tPA-treated mice ($P = .0678$). Colorimetric biochemical analysis of hemoglobin content in brain lysates (indirectly indicating the efficiency and safety of our tested thrombolytic agents) showed that SCE5-scuPA significantly reduced blood levels within the brain compared with vehicle ($P < .05$) (Figure 5B). Relative to TNK-tPA, a near-significant reduction of hemoglobin was observed ($P = .0624$). These results were notably comparable to those obtained on the CT scan (Figure 4B-C).

SCE5-scuPA preserves spleen weights and platelet numbers over time poststroke

White blood cell (WBC) counts from collected blood samples revealed that all treatment groups presented with a decrease in WBC counts from 3 to 7 days poststroke, with only SCE5-scuPA-treated

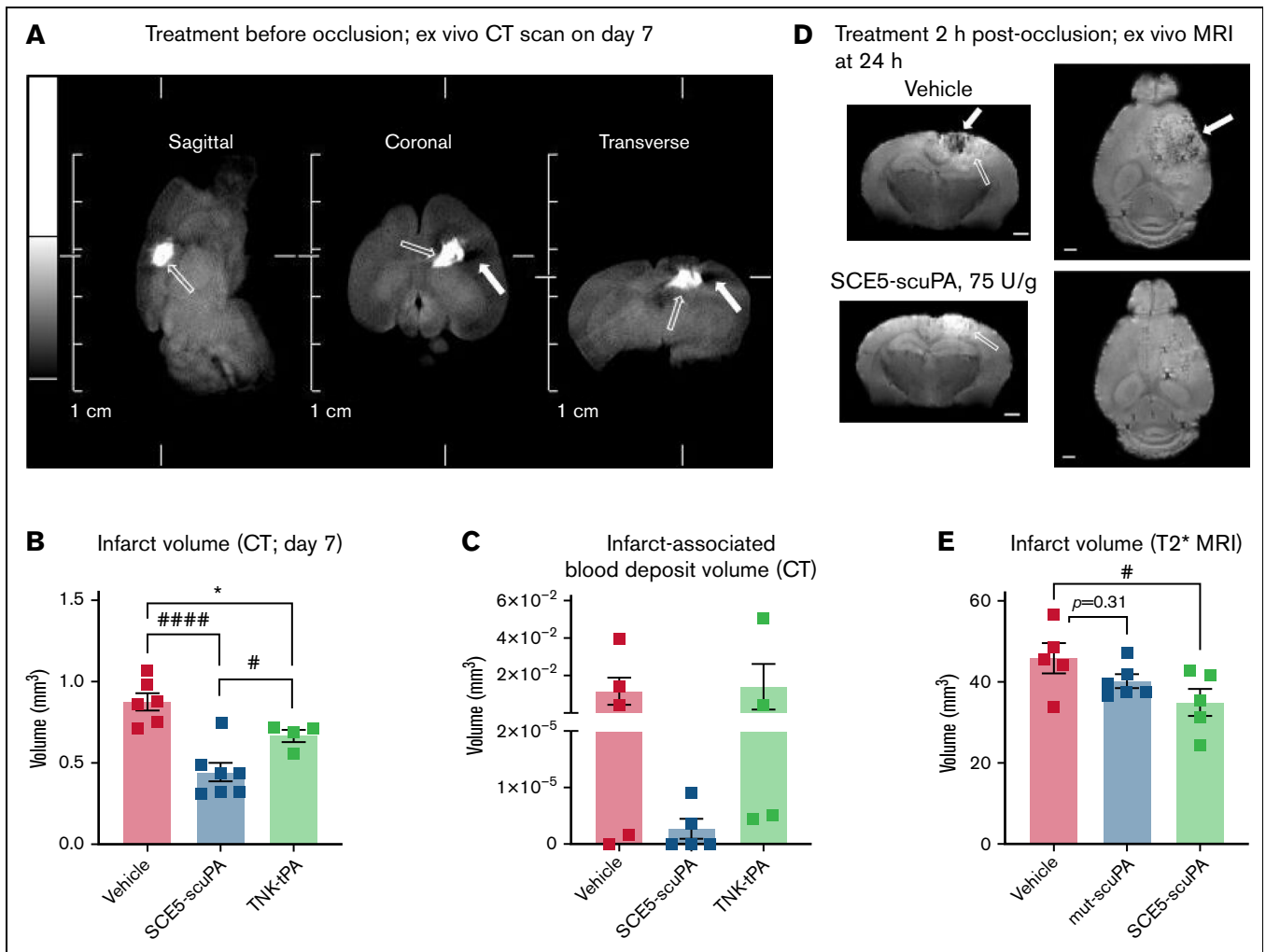


Figure 4. SCE5-scuPA treatment, either before or 2 hours post-photothrombotic stroke, reduces infarct volume and associated cerebral blood deposits. (A) Representative CT images of a mouse brain at 7 days post-photothrombotic stroke (without treatment). Solid arrows indicate hypointense (darker) voxels, consistent with low-density matter characteristic of infarcted cerebral tissue. Open arrows indicate hyperintense (brighter) voxels, representing higher density matter characteristic of blood deposits within the infarct. Scale bars as indicated on the image. (B and C) CT imaging-based quantification of infarct size (B) and blood volumes within the infarct (C) at 7 days poststroke in mice treated before photothrombotic stroke with saline (vehicle), SCE5-scuPA (150 U/g), or TNK-tPA (2.5 mg/kg). (D and E) Representative mean T2*-weighted coronal and axial MRI acquisitions at 24 hours after stroke (postmortem, intra-skull) (D) and the corresponding, MRI-based quantification of infarct size (E) in mice treated 2 hours post-photothrombotic stroke with saline (D; top panels) or SCE5-scuPA (75 U/g; D; bottom panels). Efficient clearance of blood deposits (dark areas in the vehicle-treated brain; solid arrows in panel D) and reduction in the edematous (bright; open arrows in panel D) area can be observed. Scale bars = 1 mm. Data are presented as mean \pm standard error of the mean. $\#P < .05$, $\#\#\#\#P < .0001$ by one-way analysis of variance with Tukey's or Dunnett's post hoc analysis. $*P < .05$ by a *t* test (unpaired, 2-tailed). $n = 4$ to 11.

mice exhibiting a significant decline in WBC numbers over time ($P < .05$) (Figure 5C). Although this observation may indicate some immunosuppressive effect of our fusion construct, TNK-tPA-treated mice had significantly lower spleen weight per body weight (milligrams per gram) compared with SCE5-scuPA-treated mice at 3 days poststroke ($P < .05$) (Figure 5D), suggesting that SCE5-scuPA better preserved immune function than tPA¹³ (or its TNK derivative). Furthermore, platelet counts showed that although mice treated with both thrombolytic agents maintained comparable platelet levels between day 3 and day 7, vehicle-treated mice had a significant decrease in platelet numbers over time (Figure 5E), supportive of the notion that our thrombolytic drug was in fact reducing systemic inflammation after stroke.

SCE5-scuPA utilization in a MCAo stroke model confirms its favorable safety profile

Finally, we sought to evaluate the overall safety profile and possible off-target effects of SCE5-scuPA in a thread occlusion model of the MCA. This model is ideal for safety studies of thrombolytic agents because it does not rely on clot-busting actions for brain reperfusion to occur, enabling the isolation of less desired, non-thrombolytic activities of the drug. Indeed, administration of SCE5-scuPA at reperfusion, 45 minutes after MCAo, did not worsen any of the parameters tested at 24 hours poststroke and, in fact, benefited some. More specifically, although no changes in neurologic scoring (Figure 6A), weight loss, differential blood counts

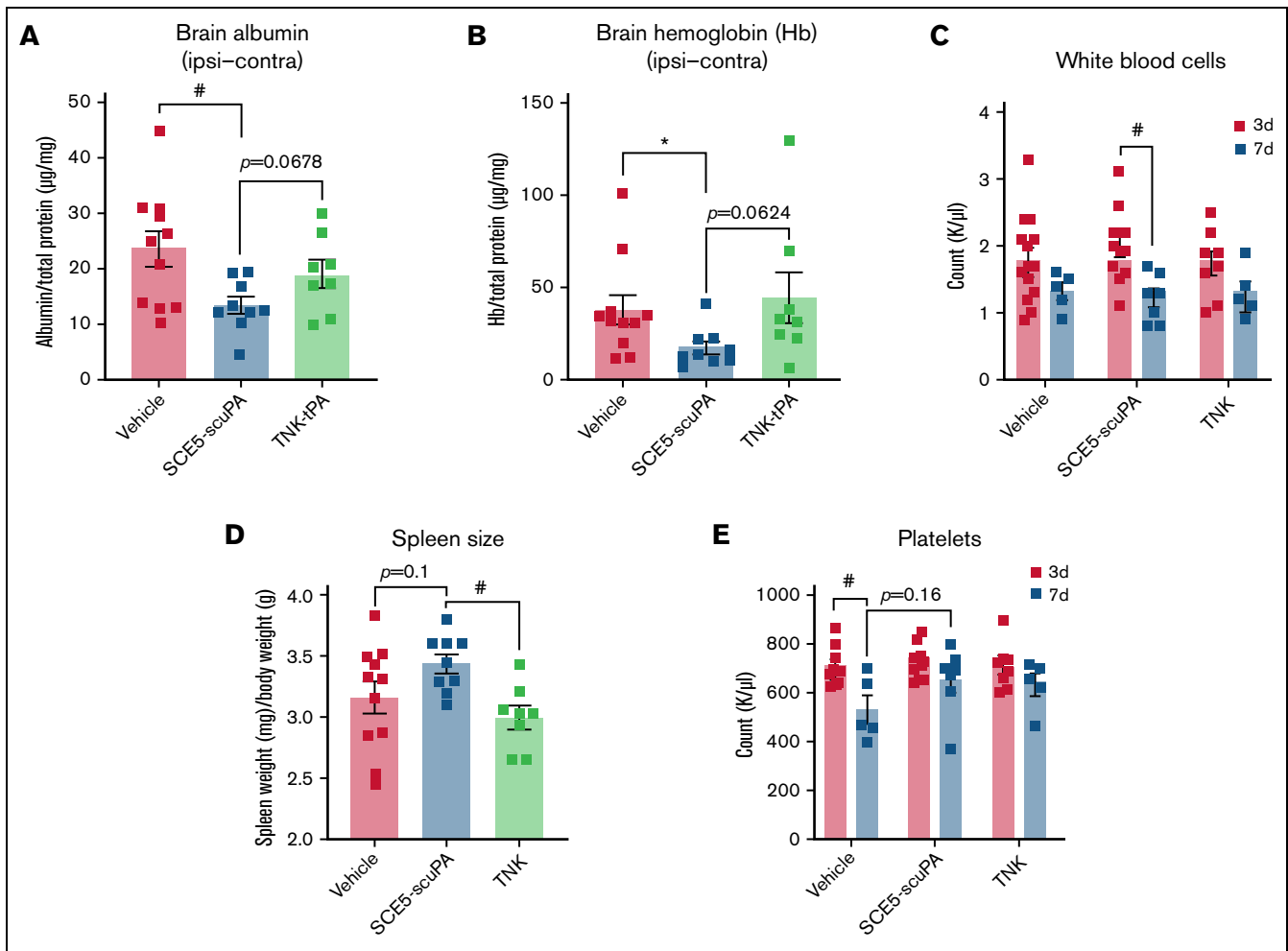


Figure 5. SCE5-scuPA protects the BBB, reduces cerebral blood content, and attenuates immunosuppression and thrombocytopenia after photothrombotic stroke. (A and B) Albumin extravasation (A) and cerebral hemoglobin (Hb) levels (B) in perfused brains 3 days after photothrombotic stroke in mice treated just before stroke with saline (vehicle), SCE5-scuPA (150 U/g), or TNK-tPA (2.5 mg/kg). The contralateral (Contra) values were subtracted from the ipsilateral (Ipsi) values to correct for perfusion efficiency. (C-E) Under the same protocol settings: WBC counts at 3 and 7 days poststroke (C), spleen size measurements at 3 days poststroke (D), and platelet counts at 3 and 7 days poststroke (E). All data are presented as mean \pm standard error of the mean. # $P < .05$ by one-way analysis of variance with Tukey's post hoc analysis. * $P < .05$ and other specified P values by a t test (unpaired, 2-tailed). $n = 5$ to 14.

(Figure 6B), or general mobility parameters on the ANY-maze (Figure 6C) were observed between saline- and SCE5-scuPA-treated sham and MCAo mice, only SCE5-scuPA did not also affect foot slips per meter; TNK-tPA seemed to worsen mice performance relative to the SCE5-scuPA and vehicle groups ($P = .063-.077$). This observation suggests that SCE5-scuPA is devoid of detrimental activities of clinically used thrombolytics that affect neurologic deficit outcomes of stroke (eg, due to a possible lack of neurotoxicity that is associated with tPA^{32,33}). Importantly, the use of SCE5-scuPA, in contrast to TNK-tPA, did not induce intracranial hemorrhage (Figure 6D) and significantly decreased (as with TNK-tPA) the brain albumin content after MCAo ($P < .05$) (Figure 6E). Furthermore, brain matrix-metalloproteinase-9 levels appeared reduced in the ipsilateral hemispheres of SCE5-scuPA-treated mice compared with their saline- and TNK-tPA-treated counterparts (Figure 6F), with no discernible changes in the plasma. These key observations show the capacity of SCE5-scuPA to protect the BBB and avoid the most feared side effect of thrombolysis, namely parenchymal

hematomas. Overall, our extensive analysis of the performance of SCE5-scuPA in the nonthrombotic, MCAo model of stroke fundamentally highlights important advantages and a sound safety profile of this novel thrombolytic when used for ischemic stroke.

Discussion

Although thrombolytic therapy with tPA continues to serve as the main emergency treatment for AIS, existing limitations present a clear clinical need to improve this life-saving intervention. The current study investigated an alternative thrombolytic agent, a recombinant fusion construct termed SCE5-scuPA, in which the plasminogen-activator uPA is fused to a single-chain antibody targeted toward glycoprotein IIb/IIIa on the surface of activated platelets (SCE5).

We proposed that the adoption of uPA as a potent, non-fibrin-dependent PA may circumvent some challenges faced by the use

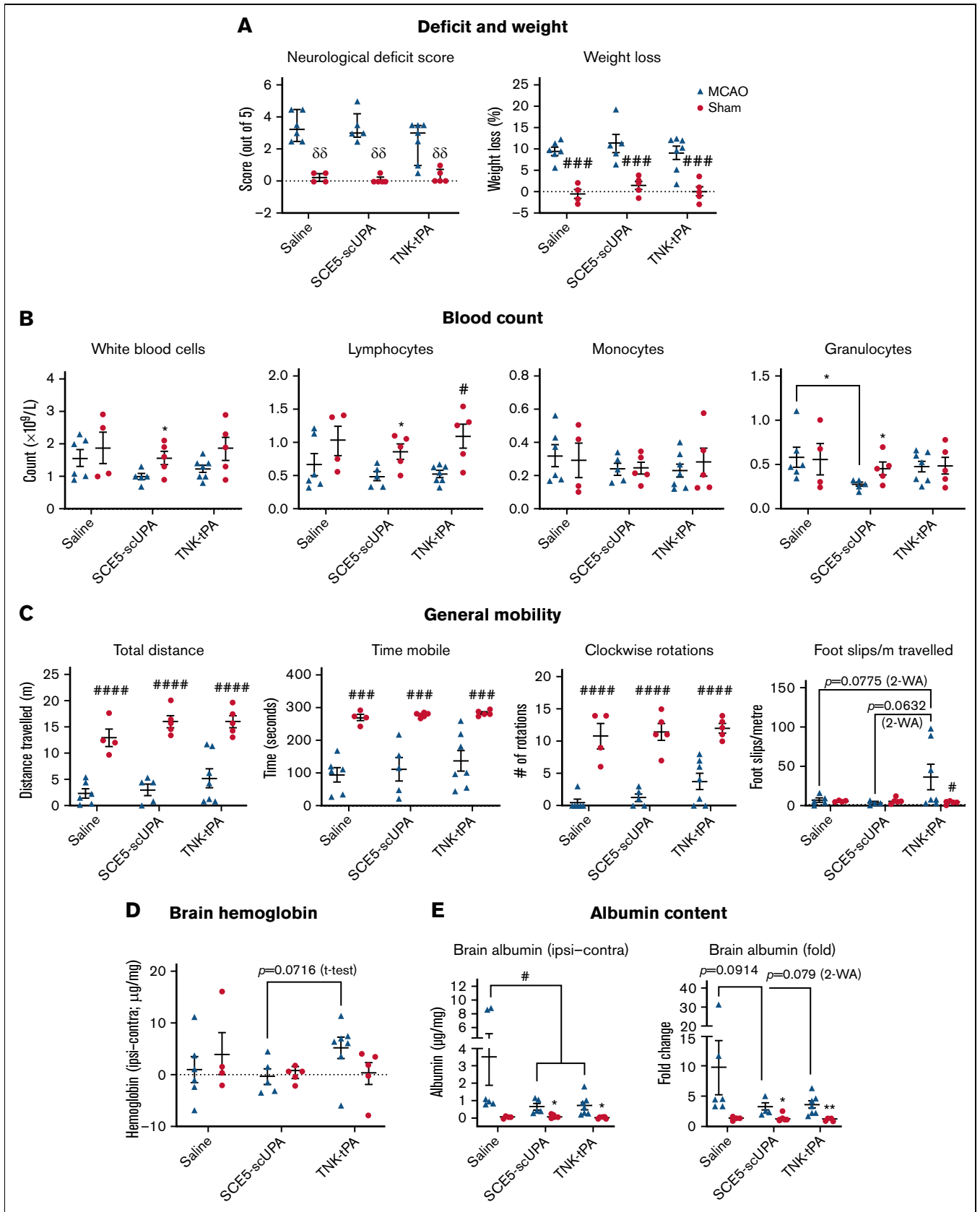


Figure 6. SCE5-scUPA is safe, protective, and lacks off-target effects in an MCAo stroke model. (A-F) Neurologic deficit scores and weight loss (A), blood counts (B), mobility parameters extracted from ANY-Maze recordings (C), brain hemoglobin content (D), brain albumin levels (E), and gelatinase (matrix-metalloproteinases [MMP]-2 and

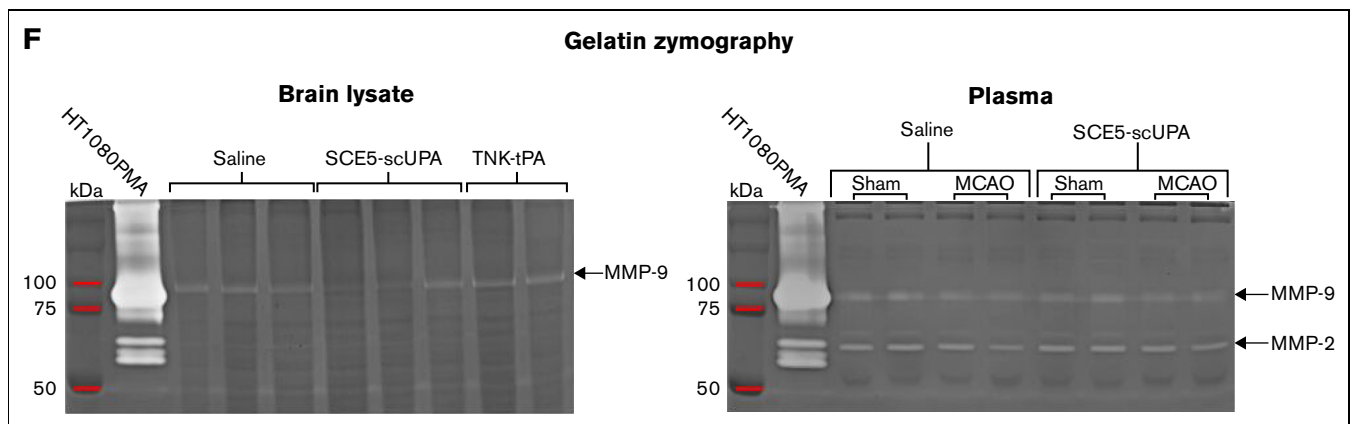


Figure 6 (continued) MMP-9) profiles (F) in brain and plasma of mice 24 hours after sham operations or 45 minutes of transient MCAo. Mice were intravenously administered at reperfusion saline, SCE5-scUPA (150 U/g), or TNK-tPA (2.5 mg/kg). SCE5-scUPA does not worsen any of the parameters tested compared with saline. Relative to TNK-tPA, SCE5-scUPA preserves motor function (panel C; right panel) and does not increase cerebral blood levels (panel D) or brain MMP-9 levels (panel F) after stroke. SCE5-scUPA and TNK-tPA both also protect the BBB (panel E). In panel D and panel E (left graph), the contralateral (Contra) values were subtracted from the ipsilateral (Ipsi) values to correct for perfusion efficiency. Neurologic scores in panel A are shown as median \pm interquartile range; $\delta\delta P < .01$ by multiple Mann-Whitney tests (unpaired, 2-tailed, corrected for multiple comparisons by Holm-Šidák post hoc). In all other panels, data are presented as mean \pm standard error of the mean; $\#P < .05$, $\###P < .001$, and $\####P < .0001$ between sham and MCAo, or as specified, by 2-way ANOVA with Tukey's or Šidák's post hoc analysis. $*P < .05$, $**P < .01$ between sham and MCAo, or as specified, by a *t* test (unpaired, 2-tailed). $n = 4$ to 5 in sham groups and 5-7 in MCAo groups. HT1080PMA, conditioned medium from HT1080 fibrosarcoma cells stimulated with phorbol 12-myristate 13-acetate (50 ng/mL) overnight, as a positive control for gelatinase activity.

of tPA, such as reliance of the latter on sufficient fibrin levels and its ability to harm neurons and disrupt the BBB. Although there is an increased risk of symptomatic intracerebral hemorrhage (sICH) associated with uPA when used to treat AIS, as shown in the PROACT II (Prolyse in Acute Cerebral Thromboembolism II) clinical trial,³⁴ we aimed to show that the active targeting of uPA to platelet-rich thrombi that is enabled in SCE5-scUPA could essentially create a “thrombi-dependent” uPA that has its bleeding risk mitigated via dose reduction. Indeed, lower doses of exogenous uPA are more likely to achieve a favorable safety profile to maintain a healthy hemostatic physiology that will not allow sICH to evolve. This is while the use of the platelet targeting SCE5 scFv would enrich the activity of the fusion construct on platelet-rich thrombi that have been clinically observed to cause AIS. The previous, extensive ex vivo and in vivo proof-of-concept investigations of SCE5-scUPA,²⁴ as well as the novel ex vivo assay presented here testing the construct on a gradient of platelets in “reconstituted bloods” (Figure 1), showed a favorable safety profile and thrombolytic efficacy that were directly attributed to its activated platelet-targeting design in general models of thrombolysis. The transition of SCE5-scUPA into treatment of AIS was therefore indicated.

From our pharmacokinetics studies, it became apparent that the fluorescently (Cy7.5)-labeled SCE5-scUPA accumulated in the liver at substantial levels, as expected.³⁵⁻³⁷ However, the higher uptake in the spleen was unexpected given that there are few to no reports supporting the clearance of uPA and targeted-uPA constructs via the spleen. It is possible that the SCE5 portion of the fusion construct was binding some circulating platelets, which were then cleared by typical, splenic platelet-clearing mechanisms³⁸; additional investigation is required, however, to understand these clearance mechanisms of SCE5-scUPA. In addition, the pharmacokinetic studies revealed that SCE5-scUPA experienced a rapid blood clearance with a circulating half-life of 3 minutes. This relatively short circulating time suggests that the optimal route of administration for SCE5-scUPA is intravenous infusion, as is

required for alteplase due to its blood half-life of 3 to 6 minutes.^{8,9} Nevertheless, this view should be balanced by the counterargument that a rapid clearance will also ensure that non-thrombus-bound SCE5-scUPA is not allowed to circulate freely for a prolonged period of time, thus minimizing the risk of bleeding complications.

For the in vivo investigation of SCE5-scUPA as a thrombolytic agent to treat AIS, we first adopted the photothrombotic model of ischemic stroke. This model presented several advantages for displaying the clinical challenges faced with administering thrombolytic therapy to treat AIS, particularly given that it yields platelet-rich clots that have shown clot lysis resistance to tPA.³⁹ In terms of the study design, several considerations were made to ensure a properly controlled study. TNK-tPA was adopted as the tPA standard-of-care comparator given its emerging gold standard status for treating patients with AIS.⁴⁰⁻⁴² Another important consideration was that the scuPA sequence was derived from human uPA and, therefore, the use of TNK-tPA, a mutated variant of human tPA, was an optimal thrombolytic control⁴³ to account for the established 10-fold reduction in affinity between mouse plasminogen and human tPA (notably, TNK-tPA was administered at 2.5 mg/kg, 10-fold of the 0.25 g/kg clinical dose). Additional controls included the nontargeted mut-scUPA at an equivalent dose of 150 U/g and the SCE5 scFv alone at 2 μ g/g, which corresponded to an equimolar dosage of SCE5 when delivered as SCE5-scUPA. Taken together, our study design allowed for a comprehensive assessment of platelet-targeted thrombolysis for the treatment of AIS.

In addition to the impressive capabilities displayed by SCE5-scUPA to improve neurologic deficits and reduce infarct size (the latter achieved with both prophylactic and poststroke, clinically relevant administration regimens), the significant reduction in extravasated albumin into the brain tissue strongly indicated that mice treated with SCE5-scUPA also benefited from a better preservation post-stroke of the BBB.^{12,44} This is while the decreased volume of blood

deposits on brain CT scans of SCE5-scuPA-treated mice favored the therapeutic potential of SCE5-scuPA, as it suggested improved thrombolysis outcomes (ie, fewer intravascular blood clots) and/or avoidance of cerebral hemorrhage poststroke. Given that vehicle-treated mice also displayed elevated cerebral hemoglobin content in brain lysates after thrombotic stroke, it is most likely that the reduced hemoglobin levels with SCE5-scuPA would be clinically associated with a lower incidence of severe side effects, such as sICH. Importantly, no ICH and preservation of the BBB were also observed in the nonthrombotic MCAo model, strengthening the notion that SCE5-scuPA has a sound safety profile in the context of AIS.

Our study was expanded to assess the potential of SCE5-scuPA to circumvent any exacerbated immunosuppressive outcomes reported with tPA treatment poststroke.¹³ Our findings in the cortical photothrombotic model showed that, on average, all treatments caused a WBC decrease at day 7 compared with day 3. This finding is supported by published studies that have shown an increased WBC count in peripheral blood shortly after stroke, followed by a decrease over time.⁴⁵⁻⁴⁷ Interestingly, Audebert et al⁴⁵ reported that successful thrombolytic outcomes poststroke were linked with a decreased WBC count in the peripheral blood over time, which coincided with minimization of neurologic deficit. This aligned with our observation that SCE5-scuPA-treated mice achieved significant improvements in neurologic deficit and were the only treatment cohort to exhibit a significant reduction in WBC count over time after brain photothrombosis. Notably, leukopenia and lymphopenia (compared with sham) were also observed in our MCAo study at 24 hours after stroke but only in the 2 thrombolytic groups (SCE5-scuPA and TNK-tPA) and not in the saline control group. This observation supports the overall conclusion that the SCE5-scuPA-associated reductions in WBCs observed in both our stroke models in fact indicate a beneficial action of this drug. Measurements of spleen weights at day 3 postcortical photothrombosis were also performed given that reduction in spleen size has been linked with immunosuppression and an increased risk of infection after stroke.⁴⁸ Our findings revealed that SCE5-scuPA-treated mice had a significantly larger splenic mass than TNK-tPA-treated mice and a (nonsignificant) increase compared with vehicle-treated mice, suggesting that mice treated with SCE5-scuPA experienced lesser immunosuppressive outcomes than other treatment groups, in line with our hypothesis.

Platelet counts were also performed at day 3 and 7 after thrombotic stroke (Figure 5E). Interestingly, only the vehicle-treated mice exhibited a significant decrease in platelet count at 7 days poststroke compared with the 3-day time points. This outcome is consistent with clinical findings showing that patients with AIS present with reduced platelet counts poststroke.⁴⁹ Promisingly, we observed that mice treated with SCE5-scuPA (and TNK-tPA) maintained comparable platelet counts between 3 and 7 days poststroke, suggesting that any adverse outcomes associated with thrombocytopenia are potentially avoided with SCE5-scuPA treatment.

Several study limitations need to be considered when interpreting the findings, particularly regarding our investigation of SCE5-scuPA in the photothrombotic ischemic stroke model. Although this stroke model offers several advantages, it is not representative of the typical stroke pathology observed in the clinic. More

specifically, this form of photothrombotic AIS produces widespread, microvascular thrombotic occlusions in the cortical region exposed to light (supplemental Figure 4). This is in contrast to clinically observed stroke cases, in which thrombi typically form within a large, single cerebral artery. Additional investigations of SCE5-scuPA could be extended to alternative preclinical stroke models that better simulate clinical stroke, as described by Sun et al.³⁹ It is worth noting that our model does draw some clinical similarities, as thrombotic events in the microvasculature occur poststroke due to blood stasis downstream of the stroke-inducing thrombus.⁵⁰

Furthermore, given the dense and extensive nature of thrombi produced by this model (supplemental Figure 4), we chose to administer the interventions in our main study before the induction of stroke. This method was used to allow each drug treatment the best opportunity to penetrate and lyse the disseminated microthrombi produced. A more limited study was performed over 24 hours with a 2-hour poststroke treatment protocol, which better resembles the clinical scenario, as thrombolytic therapy is only ever administered after thrombogenesis. The results of this “real-life” intervention were encouraging, yet mixed, with SCE5-scuPA achieving a reduction in infarct size with no improvement in neurologic deficits. One could speculate that this clinically relevant protocol may yield improved effects of SCE5-scuPA on neurologic deficit if the highest safe dose of SCE5-scuPA was used (150 U/g instead of 75 U/g) (Figure 2A) and if the evaluation was performed at a later time point (eg, 3 or 7 days), where differences could be better discerned. Although the full benefit of poststroke SCE5-scuPA administration remains to be shown, because SCE5-scuPA was also found in the MCAo model to be safe and devoid of major hemorrhagic complications (albeit at a time frame considered safe for tPA thrombolysis), our studies support the potential of this targeted drug to function also in a prophylactic manner, a capacity not currently available with any currently approved thrombolytic. In any case, our pretreatment protocol could also serve as a viable protocol for investigations of antithrombotic therapies, including novel antiplatelet agents.

In summary, our findings support the potential of SCE5-scuPA to serve as a prospective thrombolytic agent for the treatment of AIS, in which 2 functionalities, platelet targeting and potent plasminogen activation, synergize to form a safe and superior thrombolytic drug. The results presented here strongly suggest that SCE5-scuPA offers benefits across many clinical outcomes relevant to AIS, including improvement of neurologic deficit, reduction in infarct volume and brain bleeding, preservation of the BBB, and no interference with immunity and platelet numbers poststroke. Although further investigations are required to support the translation probability of SCE5-scuPA, including studies that assess its safety profile after prolonged brain ischemia (where the risk for hemorrhagic transformations increases), our findings highlight the therapeutic potential of SCE5-scuPA as a novel thrombolytic therapy for the treatment of AIS.

Acknowledgments

The authors thank the Alfred Research Alliance Flow Cytometry Core Facility, the Monash Histology platform and Monash Micro Imaging platform (all of Monash University) for their support and expertise. The authors acknowledge the facilities and scientific

and technical assistance of the National Imaging Facility, a National Collaborative Research Infrastructure Strategy capability at Monash Biomedical Imaging (a Technology Research Platform at Monash University). They also acknowledge the technical assistance of Gang Zheng, who is a National Imaging Facility Fellow, and of Bianca Jupp from the Department of Neuroscience, Central Clinical School, Monash University. The authors further acknowledge the dedicated staff of the Precinct Animal Centre for their professional assistance and animal care during this project.

This work has been funded by grant BGRF2205 by the Bethlehem Griffiths Research Foundation. Grant GNT1138361 was awarded to C.E.H. by the National Health and Medical Research Council of Australia (NHMRC). J.S.P. is kindly supported by a PhD scholarship from Australian Rotary Health and Rotary District 9830, as well as the Australian Government Research Training Program Scholarship. K.A. is a NHMRC Medical Research Future Fund Career Development Fellow (award number GNT1140465). C.E.H. is a Senior Research Fellow of the NHMRC of Australia (award number GNT1154270). B.N. is supported by NHMRC grant GNT1120129.

Authorship

Contribution: J.S.P. produced and purified the fusion construct, designed and performed the experiments, assisted in forming the concept, analyzed data, generated the figures, and drafted the

manuscript; A.A. performed experiments and analyzed data; H.H. performed experiments and provided key technical expertise; S.J. produced and purified the fusion construct; B.R.S.B. provided critical technical expertise, resources, and advice for the experimental plan; R.L.M. contributed expert knowledge and advice on the use of thrombolytics and provided thrombolytic agents and other resources; D.K.W. designed the MRI protocols and guided image analysis; K.A. performed the CT imaging, guided the analysis, and was involved in the conceptual and experimental design; C.E.H. and B.N. formed the concept, designed the experiments, supervised the work, and provided critical input in drafting the manuscript; and all authors provided input to, and approved, the final manuscript.

Conflict-of-interest disclosure: The authors declare no competing financial interests.

ORCID profiles: J.S.P., [0000-0001-5731-1246](https://orcid.org/0000-0001-5731-1246); R.L.M., [0000-0001-6885-3892](https://orcid.org/0000-0001-6885-3892); D.K.W., [0000-0002-7535-8651](https://orcid.org/0000-0002-7535-8651); K.A., [0000-0002-6252-1931](https://orcid.org/0000-0002-6252-1931); C.E.H., [0000-0002-7114-4023](https://orcid.org/0000-0002-7114-4023); B.N., [0000-0001-6714-9131](https://orcid.org/0000-0001-6714-9131).

Correspondence: Be'eri Niego, Australian Centre for Blood Diseases, Level 2, 99 Commercial Rd, Monash University, VIC, 3004 Australia; email: beeri.niego@monash.edu; and Christoph E. Hagemeyer, Australian Centre for Blood Diseases, Level 2, 99 Commercial Rd, Monash University, VIC, 3004 Australia; email: christoph.hagemeyer@monash.edu.

References

1. Johnson W, Onuma O, Owolabi M, Sachdev S. Stroke: a global response is needed. *Bull World Health Organ*. 2016;94(9):634-634A.
2. Zerna C, Thomalla G, Campbell BCV, Rha JH, Hill MD. Current practice and future directions in the diagnosis and acute treatment of ischaemic stroke. *Lancet*. 2018;392(10154):1247-1256.
3. Medcalf RL, Keragala CB. The fibrinolytic system: mysteries and opportunities. *HemaSphere*. 2021;5(6):e570.
4. Walter S, Fassbender K, Easton D, et al. Stroke care equity in rural and remote areas—novel strategies. *Vessel Plus*. 2021;5:27.
5. Hubert GJ, Kraus F, Maegerlein C, et al. The “flying intervention team”: a novel stroke care concept for rural areas. *Cerebrovasc Dis*. 2021;50(4):375-382.
6. National Institute of Neurological Disorders and Stroke rt-PA Stroke Study Group. Tissue plasminogen activator for acute ischemic stroke. *N Engl J Med*. 1995;333(24):1581-1587.
7. Gurav SK, Zirpe KG, Wadia RS, et al. Problems and limitations in thrombolysis of acute stroke patients at a tertiary care center. *Indian J Crit Care Med*. 2015;19(5):265-269.
8. Tanswell P, Seifried E, Stang E, Krause J. Pharmacokinetics and hepatic catabolism of tissue-type plasminogen activator. *Arzneimittelforschung*. 1991;41(12):1310-1319.
9. Larsen GR, Metzger M, Henson K, Blue Y, Horgan P. Pharmacokinetic and distribution analysis of variant forms of tissue-type plasminogen activator with prolonged clearance in rat. *Blood*. 1989;73(7):1842-1850.
10. Spronk E, Sykes G, Falcione S, et al. Hemorrhagic transformation in ischemic stroke and the role of inflammation. *Front Neurol*. 2021;12:661955.
11. Zhang J, Yang Y, Sun H, Xing Y. Hemorrhagic transformation after cerebral infarction: current concepts and challenges. *Ann Transl Med*. 2014;2(8):81.
12. Niego B, Medcalf RL. Plasmin-dependent modulation of the blood-brain barrier: a major consideration during tPA-induced thrombolysis? *J Cereb Blood Flow Metab*. 2014;34(8):1283-1296.
13. Draxler DF, Lee F, Ho H, Keragala CB, Medcalf RL, Niego B. T-PA suppresses the immune response and aggravates neurological deficit in a murine model of ischemic stroke. *Front Immunol*. 2019;10:591.
14. Vermeij JD, Westendorp WF, Roos YB, Brouwer MC, van de Beek D, Nederkoorn PJ; PASS Investigators. Preventive ceftriaxone in patients with stroke treated with intravenous thrombolysis: post hoc analysis of the preventive antibiotics in stroke study. *Cerebrovasc Dis*. 2016;42(5-6):361-369.
15. Bhatia R, Hill MD, Shobha N, et al. Low rates of acute recanalization with intravenous recombinant tissue plasminogen activator in ischemic stroke: real-world experience and a call for action. *Stroke*. 2010;41(10):2254-2258.

16. Lillicrap T, Keragala CB, Draxler DF, et al. Plasmin generation potential and recanalization in acute ischaemic stroke; an observational cohort study of stroke biobank samples. *Front Neurol.* 2020;11:589628.
17. Tomkins AJ, Schleicher N, Murtha L, et al. Platelet rich clots are resistant to lysis by thrombolytic therapy in a rat model of embolic stroke. *Exp Transl Stroke Med.* 2015;7:2.
18. Collet JP, Montalescot G, Lesty C, et al. Disaggregation of in vitro preformed platelet-rich clots by abciximab increases fibrin exposure and promotes fibrinolysis. *Arterioscler Thromb Vasc Biol.* 2001;21(1):142-148.
19. Stringer HA, van Swieten P, Heijnen HF, Sixma JJ, Pannekoek H. Plasminogen activator inhibitor-1 released from activated platelets plays a key role in thrombolysis resistance. Studies with thrombi generated in the Chandler loop. *Arterioscler Thromb.* 1994;14(9):1452-1458.
20. Zhu Y, Carmeliet P, Fay WP. Plasminogen activator inhibitor-1 is a major determinant of arterial thrombolysis resistance. *Circulation.* 1999;99(23):3050-3055.
21. Nordt TK, Bode C. Thrombolysis: newer thrombolytic agents and their role in clinical medicine. *Heart.* 2003;89(11):1358-1362.
22. Potla N, Ganti L. Tenecteplase vs. alteplase for acute ischemic stroke: a systematic review. *Int J Emerg Med.* 2022;15(1):1.
23. Logallo N, Novotny V, Assmus J, et al. Tenecteplase versus alteplase for management of acute ischaemic stroke (NOR-TEST): a phase 3, randomised, open-label, blinded endpoint trial. *Lancet Neurol.* 2017;16(10):781-788.
24. Wang X, Palasubramaniam J, Gkanatsas Y, et al. Towards effective and safe thrombolysis and thromboprophylaxis: preclinical testing of a novel antibody-targeted recombinant plasminogen activator directed against activated platelets. *Circ Res.* 2014;114(7):1083-1093.
25. Hagemeyer CE, von Zur Muhlen C, von Elverfeldt D, Peter K. Single-chain antibodies as diagnostic tools and therapeutic agents. *Thromb Haemost.* 2009;101(6):1012-1019.
26. Hagemeyer CE, Peter K. Targeting the platelet integrin GPIIb/IIIa. *Curr Pharm Des.* 2010;16(37):4119-4133.
27. Schwarz M, Meade G, Stoll P, et al. Conformation-specific blockade of the integrin GPIIb/IIIa: a novel antiplatelet strategy that selectively targets activated platelets. *Circ Res.* 2006;99(1):25-33.
28. Bonnard T, Law LS, Tennant Z, Hagemeyer CE. Development and validation of a high throughput whole blood thrombolysis plate assay. *Sci Rep.* 2017;7(1):2346.
29. Thirup P. Haematocrit: within-subject and seasonal variation. *Sports Med.* 2003;33(3):231-243.
30. Labat-gest V, Tomasi S. Photothrombotic ischemia: a minimally invasive and reproducible photochemical cortical lesion model for mouse stroke studies. *J Vis Exp.* 2013;(76):50370.
31. Evans MA, Lim R, Kim HA, et al. Acute or delayed systemic administration of human amnion epithelial cells improves outcomes in experimental stroke. *Stroke.* 2018;49(3):700-709.
32. Nicole O, Docagne F, Ali C, et al. The proteolytic activity of tissue-plasminogen activator enhances NMDA receptor-mediated signaling. *Nat Med.* 2001;7(1):59-64.
33. Samson AL, Nevin ST, Croucher D, et al. Tissue-type plasminogen activator requires a co-receptor to enhance NMDA receptor function. *J Neurochem.* 2008;107(4):1091-1101.
34. Furlan A, Higashida R, Wechsler L, et al. Intra-arterial prourokinase for acute ischemic stroke. The PROACT II study: a randomized controlled trial. Prolyse in Acute Cerebral Thromboembolism. *JAMA.* 1999;282(21):2003-2011.
35. Krause J, Seydel W, Heinzl G, Tanswell P. Different receptors mediate the hepatic catabolism of tissue-type plasminogen activator and urokinase. *Biochem J.* 1990;267(3):647-652.
36. Collen D, De Cock F, Lijnen HR. Biological and thrombolytic properties of proenzyme and active forms of human urokinase-II. Turnover of natural and recombinant urokinase in rabbits and squirrel monkeys. *Thromb Haemost.* 1984;52(1):24-26.
37. Zaitsev S, Spitzer D, Murciano JC, et al. Sustained thromboprophylaxis mediated by an RBC-targeted pro-urokinase zymogen activated at the site of clot formation. *Blood.* 2010;115(25):5241-5248.
38. Grozovsky R, Hoffmeister KM, Falet H. Novel clearance mechanisms of platelets. *Curr Opin Hematol.* 2010;17(6):585-589.
39. Sun Y-Y, Kuo Y-M, Chen H-R, Short-Miller JC, Smucker MR, Kuan C-Y. A murine photothrombotic stroke model with an increased fibrin content and improved responses to tPA-lytic treatment. *Blood Adv.* 2020;4(7):1222-1231.
40. Zitek T, Ataya R, Brea I. Using tenecteplase for acute ischemic stroke: What is the hold up? *West J Emerg Med.* 2020;21(2):199-202.
41. Campbell BCV, Mitchell PJ, Churilov L, et al; EXTEND-IA TNK Part 2 investigators. Effect of intravenous tenecteplase dose on cerebral reperfusion before thrombectomy in patients with large vessel occlusion ischemic stroke: the EXTEND-IA TNK Part 2 randomized clinical trial. *JAMA.* 2020;323(13):1257-1265.
42. Gao L, Moodie M, Mitchell PJ, et al; EXTEND-IA TNK Investigators. Cost-effectiveness of tenecteplase before thrombectomy for ischemic stroke. *Stroke.* 2020;51(12):3681-3689.
43. Benedict CR, Refino CJ, Keyt BA, et al. New variant of human tissue plasminogen activator (TPA) with enhanced efficacy and lower incidence of bleeding compared with recombinant human TPA. *Circulation.* 1995;92(10):3032-3040.
44. Krueger M, Härtig W, Frydrychowicz C, et al. Stroke-induced blood-brain barrier breakdown along the vascular tree—no preferential affection of arteries in different animal models and in humans. *J Cereb Blood Flow Metab.* 2017;37(7):2539-2554.

45. Audebert HJ, Rott MM, Eck T, Haberl RL. Systemic inflammatory response depends on initial stroke severity but is attenuated by successful thrombolysis. *Stroke*. 2004;35(9):2128-2133.
46. Kim JY, Park J, Chang JY, Kim S-H, Lee JE. Inflammation after ischemic stroke: The role of leukocytes and glial cells. *Exp Neurol*. 2016;25(5):241-251.
47. Furlan JC, Vergouwen MD, Fang J, Silver FL. White blood cell count is an independent predictor of outcomes after acute ischaemic stroke. *Eur J Neurol*. 2014;21(2):215-222.
48. Nous A, Peeters I, Nieboer K, Vanbinst AM, De Keyser J, De Raedt S. Post-stroke infections associated with spleen volume reduction: a pilot study. *PLoS One*. 2020;15(5):e0232497.
49. Yip HK, Chen SS, Liu JS, et al. Serial changes in platelet activation in patients after ischemic stroke: role of pharmacodynamic modulation. *Stroke*. 2004;35(7):1683-1687.
50. Grutzendler J. Angiophagy: mechanism of microvascular recanalization independent of the fibrinolytic system. *Stroke*. 2013;44(6 suppl 1):S84-S86.